Pilot-scale struvite recovery from anaerobic digester supernatant at an enhanced biological phosphorus removal wastewater treatment plant

A. Britton, F.A. Koch, D.S. Mavinic, A. Adnan, W.K. Oldham, and B. Udala

Abstract: Pilot testing of a fluidized bed reactor used to recover phosphate, in the form of struvite, from anaerobic digester supernatant was conducted at the Advanced Wastewater Treatment Plant, City of Penticton, British Columbia. The main objective of this study was to demonstrate the ability of the reactor to remove at least 70% of the phosphate in the supernatant from a digester fed with a combination of primary and secondary sludge. It was found that the operation of the reactor could be controlled to achieve any desired level of phosphorus removal up to 90%. Analysis of the recovered struvite crystals showed essentially pure struvite (>99% by weight) with small amounts of calcium (<0.5% by weight) and traces of potassium and iron. The recovered crystals had mean diameters increasing from 0.5 to 1.8 mm over the course of the study. The increasing diameters are believed to be the result of changes in the crystal structures that caused them to become stronger over the course of the study.

Key words: crystallization, nutrient removal, phosphorus recovery, struvite, sludge treatment, wastewater.

Résumé : Des essais pilotes d'un réacteur à lit fluidisé utilisé pour la récupération du phosphate, sous forme de struvite, à partir d'un surnageant d'un digesteur anaérobie, ont été effectués sur place, dans l'usine « Advanced Wastewater Treatment Plant », située dans la ville de Penticton, en Colombie-Britannique. L'objectif principal de l'étude était de démontrer la capacité du réacteur à éliminer au moins 70 % du phosphate contenu dans le surnageant d'un digesteur alimenté d'une combinaison de boues primaires et secondaires. Nous avons trouvé que l'opération du réacteur pourrait être contrôlée afin d'atteindre un niveau de récupération du phosphate pouvant atteindre 90 %. L'analyse des cristaux de struvite récupérés a montré que la struvite était essentiellement pure (>99 % poids) avec de petites quantités de calcium (<0,5 % poids) et des traces de potassium et de fer. Les cristaux récupérés avaient des diamètres moyens augmentant de 0,5 à 1,8 mm durant l'étude. Cette augmentation de diamètre est probablement causée par des changements dans la structure cristalline, solidifiant les cristaux au fur et à mesure de la progression de l'étude.

Mots clés : cristallisation, retrait des nutriments, récupération du phosphore, struvite, traitement des boues, eaux usées.

[Traduit par la Rédaction]

Introduction

Phosphorus recovery is an important area of research in the environmental engineering field. There are a variety of reasons for this, including the gradual depletion of global reserves of high-quality mined phosphate deposits and operational problems encountered in wastewater treatment plants (Niedbala 1995; Jardin and Popel 1996; Driver et al. 1999). The piping and equipment in the sludge treatment processes of these plants are increasingly prone to fouling and encrustation with struvite, thereby increasing pumping and maintenance costs. Another important factor driving this research is the increased opportunity for phosphate recovery derived from the increased use of enhanced biological phosphorus removal (EBPR). The use of EBPR in wastewater treatment leads to the creation of an enriched phosphate stream in the sludge-handling liquors (Woods et al. 1999). This enriched stream has been the focus of most investigations into the recovery of phosphorus from municipal wastewaters.

In this study, a pilot-scale phosphorus recovery reactor, developed at The University of British Columbia (UBC), was tested at the Advanced Wastewater Treatment Plant (AWWTP) in Penticton, British Columbia. This reactor was used to recover phosphate in the form of struvite ($MgNH_4PO_4 \cdot 6H_20$) from an anaerobic digester supernatant stream, through the addition of magnesium chloride and pH adjustment in a fluidized bed. The study was carried out over a 4-month period, during which time the anaerobic digester was fed with a blend of primary and secondary sludge.

Received 8 March 2004. Revision accepted 1 September 2004. Published on the NRC Research Press Web site at http://jees.nrc.ca/ on 16 July 2005.

A. Britton,[1] F.A. Koch,[2] D.S. Mavinic, and A. Adnan. Department of Civil Engineering, University of British Columbia, Vancouver, BC V6T 1Z4, Canada.
W.K. Oldham. Stantec Consulting Ltd., #1007-7445 132nd Str., Surrey, BC V3W 1J8, Canada.
B. Udala. City of Penticton Advanced Wastewater Treatment Plant, Penticton, BC, Canada.

Written discussion of this article is welcomed and will be received by the Editor until 30 November 2005.

[1]Present Address: Ostara Nutrient Recovery Technologies, Inc., #690-1199 West Pender Str., Vancouver, BC V6E 2R1, Canada.
[2]Corresponding author (e-mail: koch@civil.ubc.ca).

 doi: 10.1139/S04-059

Site selection

The City of Penticton AWWTP is one of the best-performing cold-climate EBPR plants in North America, and the staff has been extremely helpful in previous collaborative research conducted on site. The City of Penticton has also expressed an interest in being one of the pioneering municipalities in Canada with regards to implementing innovative and sustainable waste management strategies.

The AWWTP consists of preliminary treatment (including screening and degritting), primary clarifiers, two parallel modified University of Cape Town design EBPR secondary treatment trains, sand filters for secondary effluent polishing, and chlorine disinfection by chlorination and dechlorination. The City of Penticton is located in the Okanagan Valley in south-central British Columbia, between Lake Okanagan and Lake Skaha. This is a region of intense horticulture and crop irrigation and an environment sensitive to excessive nutrient input. For this reason, the wastewater treatment plant is subject to very low effluent phosphorus standards (0.25 mg/L PO_4-P). The sludge treatment train for this plant consists of primary sludge fermenters that provide the required volatile fatty acids for the EBPR system and a two-stage anaerobic digester for the fermented primary sludge. The digested sludge is then dewatered on a belt press after being combined with thickened waste-activated sludge (WAS) from the EBPR trains. The WAS is not digested on site because this practice leads to the release of the excess phosphorus in the sludge from the EBPR system (Niedbala 1995; Mavinic et al. 1998). Instead, the combined dewatered sludge is composted off site in windrows at the municipal landfill, and the composted sludge is sold as a soil conditioner to local landscaping and agricultural operations. During the course of this study, the operation of the sludge treatment system was modified to transfer a portion of the thickened WAS to the digester to obtain a digester supernatant stream rich in phosphate and ammonia.

Research objectives

The main purpose of this study was to use real supernatant to test the reactor at a full-scale EBPR wastewater treatment plant. Previous research at UBC had successfully demonstrated a reactor design used to recover struvite from synthetic supernatants with Mg, NH_4-N, and PO_4-P concentrations similar to those expected in the digester supernatant at the City of Penticton AWWTP; however, some concerns remained as to the effects of dissolved constituents and suspended solids in the real supernatant on the control and operation of the reactor. Both bench- and pilot-scale experiments had been conducted at UBC prior to this on-site study, and the expected operating parameters were determined prior to setting up the pilot plant at Penticton (Dastur 2001; Adnan et al. 2003*a*).

The prime objective of this study was to determine the operational parameters that would allow successful operation of the pilot-scale reactors treating real anaerobic digester supernatant from a full-scale EBPR wastewater treatment plant. Successful operation was defined as the controlled removal of at least 70% of the orthophosphate from the digester supernatant and the recovery of this phosphorus in the form of large (>1 mm) and easily separable struvite crystals.

Fig. 1. Pilot-scale struvite crystallizer reactor process design.

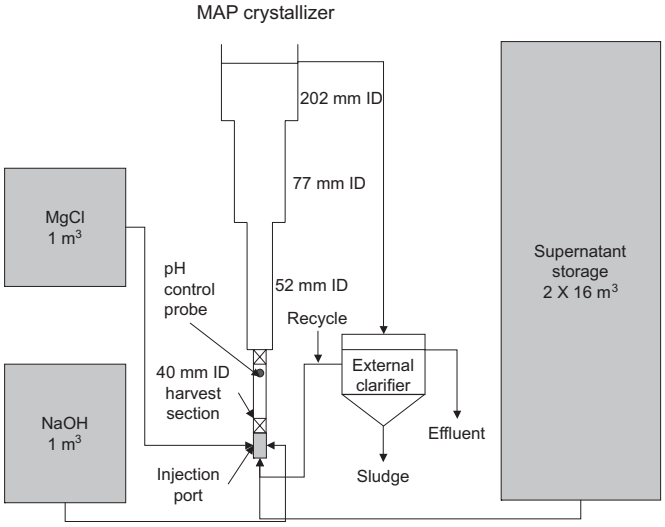

Materials and methods

Reactor design, process description, and operation

Based on previous experiments at the bench scale, a pilot-scale reactor was designed and tested at the UBC Environmental Engineering Pilot Plant using a synthetic feed (Adnan et al. 2003*a*). Two identical reactors based on this design were installed and operated in parallel over a 4-month period, from September to December 2001, at the City of Penticton AWWTP. They were housed in an on-site, heated chemical storage building.

Figure 1 shows the basic design of the reactor and associated equipment. The reactor itself was a fluidized bed reactor with sections of increasing diameter and a settling zone at the top. The diameter changes caused turbulent eddies above each transition, ensuring that sufficient mixing existed in the reactor, and also helped to classify the fluidized particles by size. Only the largest crystals in the reactor were harvested.

The crystallizer was constructed of clear PVC piping connected with standard fittings. The inside diameters were 40, 52, and 77 mm, respectively, for the bottom, middle, and top sections of the fluidized zone. The clarifier section at the top of the crystallizer was built out of 202-mm-diameter clear acrylic pipe. The total liquid volume of each reactor was approximately 19 L, 9 L of which were in the three fluidized zones. The total height of the reactors was approximately 4900 mm. The total liquid flow rate through each reactor for the duration of the study was 3.6 L/min. Each reactor was equipped with two pH probes, one in the top of the harvest zone and another in the external clarifier. The main function of the external clarifier was to recycle the effluent back into the reactor. It was also used to

trap the washed-out fine crystals from the reactor. A stainless steel injection port was provided at the base of the reactor to blend the influent, recycle, and chemical-dosing streams.

The pH probe in the harvest zone, with a proportional flow pH controller, was used for feedback control. Magnesium was dosed to the reactor in the form of magnesium chloride solution to supply the desired magnesium to phosphorus molar ratio in the reactor.

Chemicals, storage tanks, and pumps

The digester at the City of Penticton AWWTP is a two-stage anaerobic digester, operated in the mesophilic (36−40 °C) temperature range. The first stage of the digester is gas mixed; the second stage is unmixed. Supernatant from the second stage of the digester was pumped from an overflow splitter box into two storage tanks for use in the pilot struvite crystallizer. Each tank had a capacity of 16 000 L and was equipped with overflows and drain valves. The supernatant was pumped out of the tanks from a fitting located approximately 500 mm above the tank bottom; this allowed any suspended solids in the supernatant to settle to the bottom of the tank and prevented excess solids from entering the reactor. One full tank would typically last approximately 7 d when feeding both reactors.

The large volume of the storage tanks also allowed a constant feed strength to be maintained for several days at a time. This was crucial during the initial months of the study, when the supernatant characteristics were changing significantly on a daily basis. Feed supernatant was pumped from the storage tanks using a Moyno™ model 500 331 progressive cavity pump, with a 1/2 HP AC motor and variable frequency drive, to allow precise flow control (capacity 0.3–7.6 L/min). Each reactor had its own independent pumping system to ensure accurate flow control and to allow different types of operation to be evaluated in parallel.

Because the solubility of struvite is highly pH dependent (Abe 1995; Doyle et al. 2000), a pH control system is critical to maintain the desired supersaturation conditions in the crystallizers. For this study, the pH was adjusted using sodium hydroxide (caustic soda). The pH in the reactor was monitored at the top of the harvest zone (as shown in Fig. 1) using a Cole-Parmer double-junction, in-line pH probe. The pH was controlled based on this signal using a Cole-Parmer model EW-56025-40 pH control system with proportional output.

Magnesium was found to be the limiting reagent in the formation of struvite from the Penticton digester supernatant; thus, it was necessary to supplement the reactor with magnesium. Throughout this study, the objective was to keep a molar ratio of Mg:PO_4-P equal to 1.3:1 within the reactor. This higher magnesium concentration causes the limiting reagent to be phosphate and thus allows for lower effluent phosphate concentrations than in magnesium-limited systems. A Mg:PO_4-P ratio of 1.3:1 was previously found to reliably provide low-effluent phosphorus concentrations while allowing large crystals to be grown in previous bench-and pilot-scale studies (Dastur 2001; Adnan 2002). In this study, the magnesium requirements were met using a solution of magnesium chloride hexahydrate.

Sampling and analyses

Samples of the digester supernatant and the effluent from each reactor were collected daily and subsequently filtered and analyzed for total magnesium or $[Mg^{+2}]_{total}$, total ammonia–nitrogen or $[NH_4\text{-}N]_{total}$, and total orthophosphate or $[PO_4\text{-}P]_{total}$. All samples were filtered using Fisherbrand G6 filter papers with a nominal pore size of 1.5μm to remove suspended solids from the samples. $[Mg^{+2}]_{total}$ was analyzed using flame atomic absorption spectrophotometry (model Varian Inc. SpectrAA220™ fast sequential atomic absorption spectrophotometer). Calcium, aluminum, iron, and potassium analyses were performed on the samples from the crystal product analysis. These analyses were also performed by atomic absorption spectrophotometry. On-site ammonia tests were performed with a Hach DR2000 spectrophotometer, using the salicylate method (Hach, Nitrogen, Ammonia, High Range Test'N Tube™ method 10031). Orthophosphate was measured on site using the stannous chloride method, as described in method number 4500-P D in *Standard Methods for the Examination of Water and Wastewater* (APHA/AWWA/WEF 1995), with the exception that sample sizes were 50 mL instead of 100 mL. Sample absorbances were measured using a Milton Roy Spectronic 401 spectrophotometer.

Crystal harvest procedure

Crystals were harvested from the reactor after the feed, recycle, and chemical feed flows were stopped, and the crystals were allowed to settle. The harvest zone (see Fig. 1) was isolated using ball valves after the settling was complete, and the settled bed volume of struvite crystals was measured. To remove the crystals for harvesting, the injection-port section of the reactor was removed and the crystals were allowed to fall into a bucket. The harvest zone was then rinsed with reactor effluent to ensure that all crystals were removed. The harvested crystals were then air dried before analysis.

Crystal product analyses

Samples of several of the harvested crystals were dissolved in a 0.5% nitric acid solution to determine the composition and purity of the crystals grown in the reactor. These solutions were subsequently analyzed for the components of struvite, as well as calcium, aluminum, iron, and potassium. For each sample analyzed, a known weight of struvite crystals (approximately 30 mg) was dissolved in 50 mL of 0.5% nitric acid solution. To accelerate the crystal dissolution, the samples were submerged in an ultrasonic bath until no visible solids remained. Samples were then inverted several times and vortex mixed before analysis.

Struvite solubility determination

The solubility product or K_{sp}, as defined in this study, is the product of the ionic activities of the precise ionic forms involved

in the formation of a precipitate. For struvite, this relation is defined by eq. [1], where the { } braces indicate ion activity in moles per litre.

$$[1] \qquad K_{sp} = \{Mg^{2+}\}\{NH_4{}^{+}\}\{PO_4{}^{3-}\}$$

The problems associated with using K_{sp} for reactor control has been discussed elsewhere (Britton 2002; Adnan et al. 2003*b*). A more practical way to operate the reactor is to use the concept of conditional solubility product (Snoeyink and Jenkins 1980; Ohlinger 1999; Britton 2002; Adnan et al. 2003*b*). The struvite conditional solubility product (P_s), as employed in this study, is the direct product of the analytical results for soluble magnesium, ammonia nitrogen, and orthophosphate, as defined by eq. [2], where the [ ] brackets indicate concentration in moles per litre.

$$[2] \qquad P_s = [Mg^{2+}]_{total}[NH_4 - N]_{total}[PO_4 - P]_{total}$$

An equilibrium conditional solubility curve was developed using the digester supernatant from the City of Penticton AWWTP, over a range of pH values. This curve was developed for use as a control parameter for struvite crystallization at the pilot scale (Britton 2002).

Apparatus

The apparatus used for determining the solubility of struvite was a six-station paddle stirrer (Phipps and Bird). Square jars containing 1.5 L of the solution being tested were immersed in a constant temperature bath at 20 ± 0.1 °C. The paddle stirrers were set to operate at 70 ± 2 rpm. A sufficient mass of struvite crystals, harvested from the reactors, was placed in each jar to ensure that some solid-phase struvite remained at equilibrium. Equilibrium was assumed to be reached 24 h after conditions were changed in each jar, as shown by previous research at UBC (Adnan et al. 2003*a*). The pH in each jar was adjusted using dilute hydrochloric acid and sodium hydroxide solutions to determine the solubility of struvite over the expected operating range of struvite crystallization equipment (i.e., between pH 7 and 9). After 24 h for a given set of conditions, the pH and conductivity in each jar were measured. Conductivity was measured using a Hanna Instruments HI9033 multi-range conductivity meter. Samples were filtered using 0.45-μm Whatman filter paper, preserved, and later analyzed for magnesium, ammonia-nitrogen, and orthophosphate, according to the analytical methods described earlier. It should be noted that for the 24-h equilibrium period, it was assumed that the struvite was pure and crystal size did not affect struvite solubility to any extent.

Terminology

Feed supersaturation ratio

The feed or influent supersaturation ratio (SSR) describes the hypothetical SSR that would exist in an instantly mixed solution consisting of digester supernatant, magnesium chloride, and sodium hydroxide, in proportions equal to those fed to the reactor. The SSR was calculated based on eq. [3], where $P_{S\ sample}$ represents the calculated conditional solubility product of the sample being analysed and $P_{S\ equilibrium}$ represents the equilibrium conditional solubility product for that same sample, based on an equilibrium conditional solubility curve developed as described above.

$$[3] \qquad SSR = P_{S\ sample}/P_{S\ equilibrium}$$

In-reactor supersaturation ratio

The SSR in the reactor was calculated using the same methodology as the feed SSR; however, in this case $P_{S\ sample}$ is calculated by combining the concentrations of magnesium, ammonia, and orthophosphate in the reactor feed and recycle streams. Therefore, it is representative of the SSR in a completely mixed sample drawn from immediately above the injection ports of the reactors.

Recycle ratio

The recycle ratio represents the ratio of the flow from the recycle pump to the combined flow from the supernatant feed pump and chemical-dosing pumps. This recycle ratio is used to control the in-reactor SSR by diluting the feed with treated effluent. Details on this method of controlling reactor operations are provided elsewhere (Britton 2002; Adnan et al. 2003*b*).

Crystal retention time

The concept of crystal retention time (CRT) was developed by the UBC project team to quantify the crystal age (i.e., the average time the crystals spend in the reactor). Analogous to the concept of solids retention time in an activated sludge process, details on CRT calculation can be found elsewhere (Britton 2002; Adnan et al. 2003*a*).

Mean crystal size

The mean crystal size of each harvest was calculated by sieving and weighing each size fraction of the dried struvite crystal product. All the crystals in each size fraction were assumed to be of a diameter in the middle of the size range. For example, the crystals that were <0.5 mm were assumed to be 0.25 mm in diameter, the 0.5–1-mm crystals were assumed to have a diameter of 0.75 mm, and so on.

Percent phosphate removal

Because the removal of phosphorus was a primary objective of this research, the percentage of phosphate removed from the digester supernatant stream was monitored. This was calculated based on a mass balance on phosphorus around the reactor (Britton 2002).

Results and discussion

The reactor design described in this paper was successful in recovering phosphate in the form of struvite from a full-scale digester supernatant at the City of Penticton AWWTP. Crystalline product was recovered from the reactor as small pellets, with average diameters approaching 2 mm by the end of the

Fig. 2. Struvite pP_S in digester supernatant and distilled water as a function of pH.

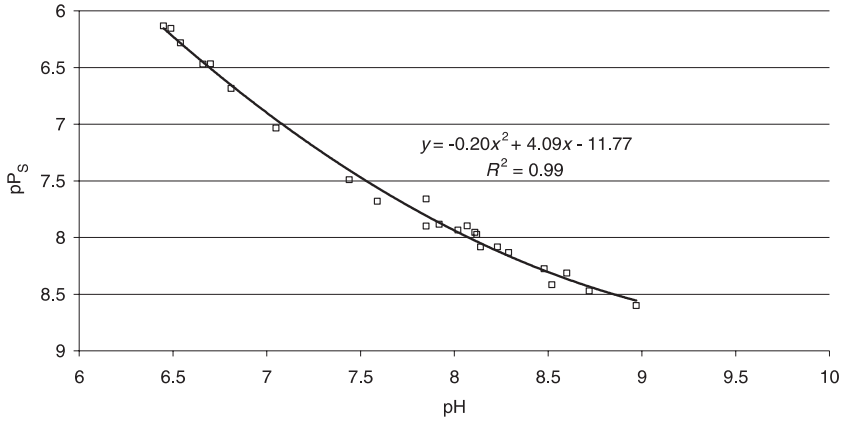

study. These crystals were found to be nearly pure struvite and of a hardness adequate to allow easy separation and processing of the product.

The overall operation period of the reactors was from 2 September to 13 December 2001. However, because of the low phosphate (PO_4-P) content (7.8–18.8 mg/L) in the digester supernatant initially, the operation of the reactors before 12 October 2001 was essentially a commissioning phase and little phosphorus recovery was possible. During this time, high chemical dosages of both magnesium chloride and sodium hydroxide were necessary to induce the crystallization of struvite. These early data are not presented here, other than to say that phosphate removal to <5 mg/L by struvite crystallization is possible but at a high operating cost.

Struvite solubility product determination

Several authors have attempted to determine a solubility product for struvite, but there is a wide range of reported solubility values (Dastur 2001). Therefore, it was considered important for this study to determine the equilibrium conditions that could be expected, when treating real digester supernatant from the Penticton AWWTP.

Thermodynamically, there should be a single value of K_{sp} that should apply to all solutions, as long as it is possible to determine the activity of each chemical species accurately. Unfortunately, this is difficult to do for individual compounds in digester supernatant because of the presence of a myriad of known and unknown compounds. The presence of these compounds also leads to a wide range of possible competing reactions, which could skew the solubility product determination.

Struvite conditional solubility product

As a simple means of determining the saturation state of the supernatant being treated, a well-defined concept of P_S was used (Ohlinger 1999; Britton 2002; Adnan et al. 2003*b*). Figure 2 shows the experimentally determined struvite P_S curves for digester supernatant. A second order polynomial curve was fitted to the data using Microsoft Excel software, and this curve was used subsequently to represent equilibrium conditions in the solutions. For the supernatant curve, eq. [4] describes this polynomial curve, where pP_S is the negative logarithm of the P_S. This curve fits the data with a R^2 value of 0.993, indicating that this is an accurate representation of the equilibrium conditions in this particular supernatant.

$$[4] \qquad pP_s = -0.203pH^2 + 4.09pH - 11.76$$

Supernatant characteristics during the study

The operation of the digester at the City of Penticton AWWTP was modified during the course of this study. This resulted in significant changes to the composition of the supernatant from the digester. Normal operation of the digester involved only the digestion of primary sludge, resulting in PO_4-P concentrations of 5–15 mg/L in the digester supernatant. At the beginning of the study (early September), the digester was supplemented with thickened WAS from a thickener tank. This practice appeared to hydraulically overload the digester, resulting in suspended solids concentrations of up to 2000 mg/L in the supernatant, and it was therefore discontinued until a better solution could be found.

Following this period, a method of transferring WAS from the gravity belt thickener was devised, thereby allowing the transfer of much thicker sludge (approximately 5% solids). This practice allowed much more WAS to be transferred to the digester without hydraulic overloading, and the phosphate concentration could increase without high suspended solids in the supernatant. Once this practice was established in early October, it was possible to maintain much higher phosphate concentrations in the digester, as can be seen in Fig. 3. The concentrations of ammonia and phosphate increased steadily as the WAS content in the digester was increased. However, the magnesium concentration remained relatively constant and independent of the ammonia and phosphate concentrations; this is contrary to the belief that magnesium is released in conjunction with phosphate when EBPR sludge is digested anaerobically (Doyle et al. 2000; Jardin and Popel 2001). The reasons for this different trend were not investigated as part of this study, but they are under investigation in follow-up work.

From 12 October to 13 December, the concentration of PO_4-P ranged from 37 to 71 mg/L, whereas the NH_4-N concen-

Fig. 3. Digester supernatant composition.

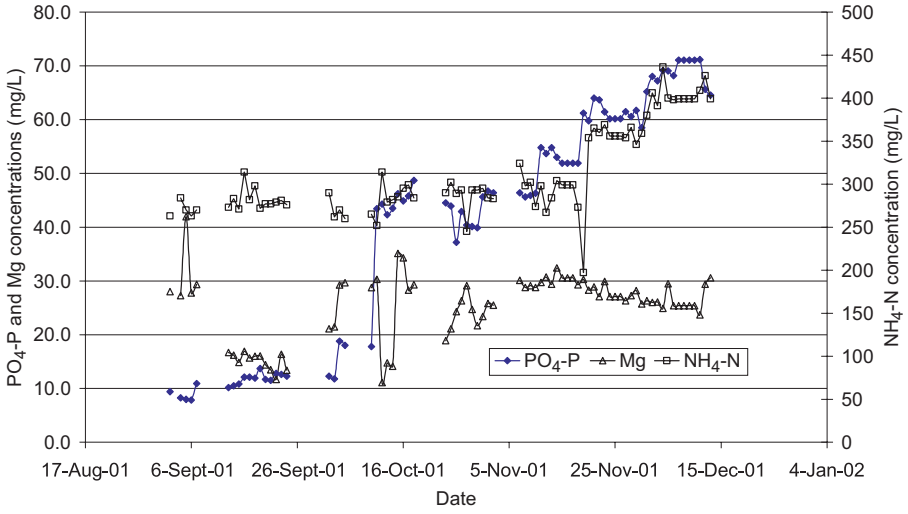

Fig. 4. Percentage phosphate removal for each reactor.

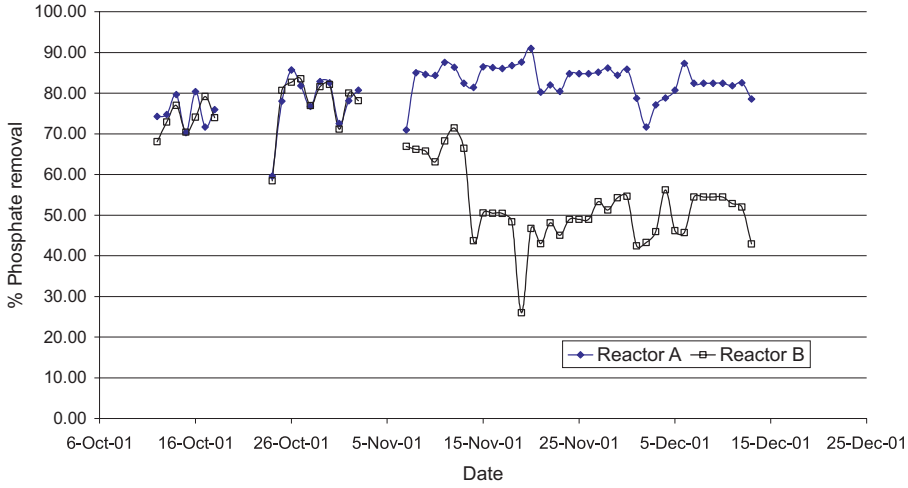

tration ranged from 197 to 436 mg/L and the Mg concentration ranged from 11 to 35 mg/L. Because of the wide variation in the composition of the supernatant being fed to the crystallization reactors, the operation of both reactors was continually modified as needed to maintain stable crystal growth conditions in the reactor.

Reactor operation

In general, the reactors operated as expected and in a manner similar to the operation observed during previous trials with similar, pilot-scale reactors using synthetic supernatant (Adnan et al. 2003*a*). The crystals harvested from the reactor were generally of a darker colour and of a smaller diameter than those harvested from synthetic supernatant; however, removal and recovery of these crystals were easy and the product-handling methods used in the previous trials worked well here.

Phosphate removal efficiency

One of the main objectives of this research was to remove phosphate from the digester supernatant stream in a full-scale EBPR plant. Overall, it was possible to control the phosphorus removal efficiency within the range of 30% to 90%. This control was exerted either by setting the pH in the reactors or by setting the inlet SSR. The original objective of the study was to demonstrate that it was possible to remove at least 70% of the orthophosphate from the digester supernatant. Figure 4 presents the orthophosphate removal efficiencies achieved during the study, demonstrating adequate removal control.

Variations from the target value were investigated to compare the economics of different removal efficiencies. The two reactors were operated in a parallel until 7 November, when the operation of reactor B was modified to purposely achieve lower orthophosphate removal. This was done by reducing pH, which lowered the inlet SSR, while maintaining the same Mg:PO_4-P molar ratio as reactor A. With the exception of 1 d, when the magnesium feed to the reactor was accidentally interrupted (24 October), the removal of orthophosphate in reactor A was maintained above 70%. This shows that it is possible to maintain the removal efficiency targeted in this study and that it was possible to maintain a higher removal efficiency if desired

Fig. 5. Phosphate removal vs. operating pH in the struvite crystallizing reactors.

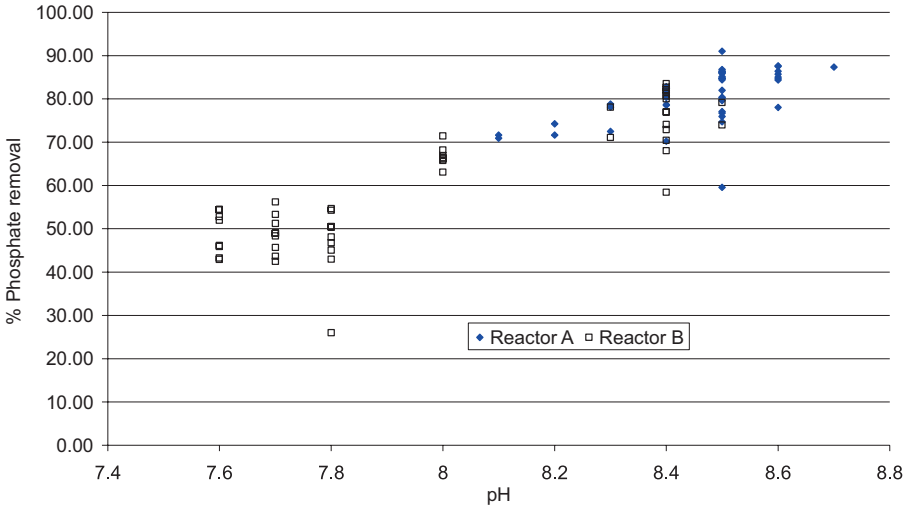

Fig. 6. Phosphate removal vs. inlet supersaturation ratio.

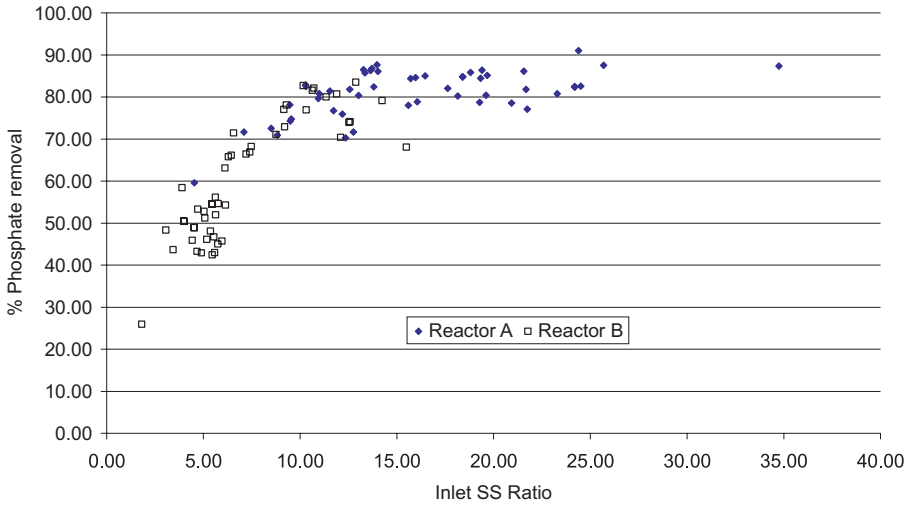

(>80%) for a supernatant with an orthophosphate concentration of at least 40 mg/L. These results are consistent with results obtained in several other studies where struvite was being recovered from full-scale digester liquors (Abe 1995; Munch and Barr 2001; Ueno and Fujii 2001).

For orthophosphate removal, two possible factors were evaluated to control the percentage removal: the operating pH of the reactor and the inlet SSR. The first assumes that the variation in the Mg:NH_4-N:PO_4-P molar ratios in the supernatant is small and can therefore be ignored; also, the percentage of phosphorus removed will vary with the operating pH, simply because the solubility of struvite, as defined by the equilibrium P_S, varies with pH. This method of evaluation is by far the simplest and is useful for the day-to-day operation of the reactor; however, it would probably fail to predict accurately the performance of a reactor at a new site with different molar ratios. This relation is shown graphically in Fig. 5. The wide range of removal efficiencies for a given pH (up to 31%) is due to the change in inlet concentrations and changes in the Mg:NH_4:PO_4 molar ratios during this study. In other words, this method of prediction is useful, but simplistic, and would not be adequate for a supernatant that is highly variable in composition if precise control of the orthophosphate removal is required.

In the second method of predicting the removal of orthophosphate, the inlet SSR is used. This method assumes that the effluent is at equilibrium. Therefore, it is possible to predict the effluent phosphate concentration by assuming equimolar removal of Mg, NH4-N, and PO_4-P. Figure 6 shows the percentage of phosphorus removal versus the inlet SSR for the operating period in both reactors. The important factors that contribute to the scatter in Fig. 6 are the inaccuracies in the measurement of the Mg, NH_4-N, and PO_4-P concentrations, as well as in the measurement of the pH. The fact that a SSR is a function of all four of these measured values makes for a compounded error,

Table 1. Comparison of theoretical struvite production based on cumulative daily orthophosphate removal and actual struvite recovery based on cumulative struvite harvest weights during the 3-month study period.

	Reactor A	Reactor B
Cumulative struvite harvested (kg)	7.82	6.50
Struvite left in reactor at end of study (kg)	3.80	4.35
Total struvite recovered (kg)	11.62	10.85
Theoretical struvite produced (kg)	13.54	12.52
Struvite recovered (%)	86	87

but the advantage is that this method allows the prediction of removal efficiency in a widely varying supernatant composition, with the same accuracy.

Overall, the best method to use to predict phosphate removal from an operational point of view will depend on the degree of accuracy wanted and the available data. A reactor can be controlled to remove the desired amount of phosphate by varying the operating pH or the inlet SSR. The difference between the two methods is that the first takes into account only one of the factors involved and may be applicable only for a specific supernatant, while the latter requires a more complete analysis of the situation and is more generally applicable.

Struvite recovery

To ensure that the phosphate being removed from the supernatant was being recovered, the dry weight of each harvest of struvite was recorded, and the final dry weight of struvite in each reactor was recorded at the end of the experiment. These masses were compared with the theoretical mass of struvite that should have been formed, based on the phosphate removed from the digester supernatant (see Table 1). The struvite considered to be recovered is the mass weighed after the drying and sieving of the harvested product. Some losses occurred during the process of harvesting, drying, transferring, sieving, and weighing the product struvite crystals. Another source of error is that this analysis assumes that the reactors were operating 24 h a day, when in fact they were shut down daily to harvest crystals, monitor collapsed bed depth of crystals, clean injector ports, and calibrate pH probes. On average, these shutdown periods were estimated to be 1 h per day or 4% of the time.

Table 1 shows that between 86% and 87% of the phosphate removed was recovered. Correcting these values for the estimated shutdown time brings the theoretical recovery rates to between 90% and 91%. If the relatively small mass of struvite produced and the amount of handling and process losses over the three months of this study are taken into account, the recovery was higher than expected. In a full-scale crystallization installation, it is expected that the losses would represent a smaller fraction of the produced struvite because of the larger scale involved.

Supersaturation ratio

Figures 7 and 8 show the feed, in-reactor, and effluent SSRs for reactors A and B, respectively. The most notable difference between the SSRs in Figs. 7 and 8 are in the influent SSRs. This is because of the lower targeted recovery in reactor B. Because reactor B was operated at a lower pH, while the same $Mg:PO_4$-P molar ratio as reactor A was maintained, the influent SSR was lower in reactor B. This allowed more supernatant to be pumped through the reactor at a lower recycle ratio, while the same struvite crystal growth rate or struvite loading rate was maintained. Overall, by maintaining relatively constant struvite loading rates in both reactors, the in-reactor SSRs and the effluent SSRs remained similar in both reactors.

Struvite product characteristics

Three major characteristics of the harvested struvite crystals were investigated: size, apparent density, and chemical composition. The crystals were also examined microscopically, both by optical microscope and by scanning electron microscope (SEM).

Struvite crystal size

In general, the size of the harvested crystals continuously increased during this study, even after several complete reactor volumes had been harvested. Figure 9 shows the mean crystal diameter of each harvest from both reactors. With time, the crystals grew stronger and larger. One of the most important factors in determining the final diameter of the crystals was their structural strength. The early crystals tended to break easily during the harvesting, drying, and sieving operations, whereas the crystals harvested late in this study did not tend to break much during the subsequent handling processes.

These results imply that several complete CRTs must elapse before a steady-state crystal size will be reached, as suggested by Takiyama et al. (1997). In fact, the mean crystal diameters shown in Fig. 9 do not appear to be approaching their steady-state values, even after 2 months of operation. Similar results were reported by Abe (1995). Further, longer term studies would be necessary to determine the final steady-state size the struvite crystals can be expected to reach. From the data collected in this study, the mean crystal diameter grew by an average of 0.016 mm per day.

Struvite crystal bulk density

Although the density of the crystals was not measured directly in this study, an interesting trend was observed in the mass of crystals removed from the harvest section of the reactor with time. For each harvest, the flow through the reactor was stopped and the fluidized crystals were allowed to settle before the harvest zone was isolated using ball valves and the crystals were withdrawn from the reactor. In this manner, a constant volume of approximately 1.1 L of crystals was harvested each time. It was noticed throughout the study that the crystal mass harvested from this volume consistently increased with time. Figure 10 shows this trend.

The first harvests in the study had a total mass of approximately 200 g, whereas the final harvests had a mass of approximately 600 g. This trend did not appear to reach a maximum by the end of this study. In general, the crystal mass harvested

Fig. 7. Reactor A supersaturation ratios.

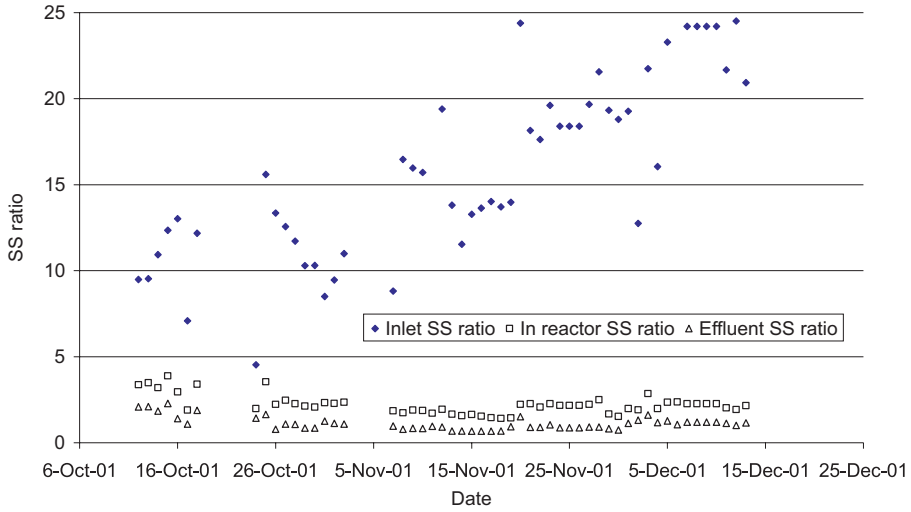

Fig. 8. Reactor B supersaturation ratios.

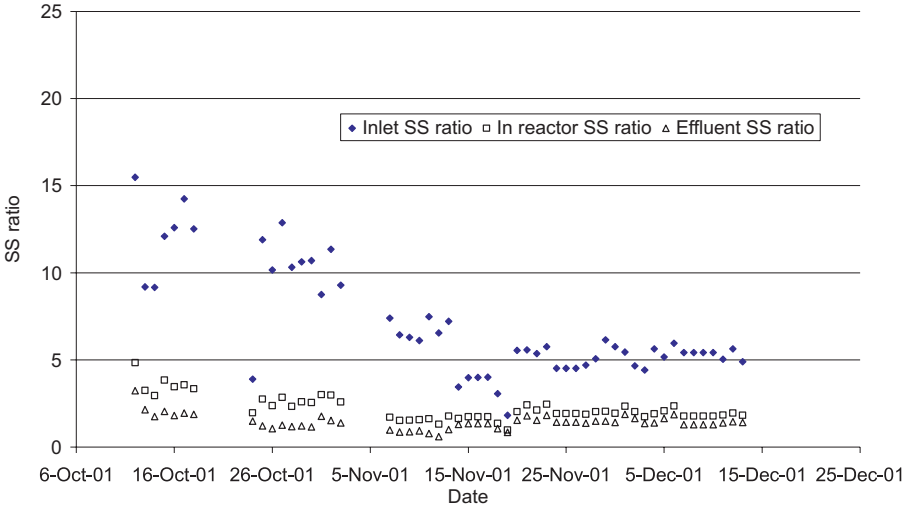

Fig. 9. Mean crystal diameter of struvite crystals harvested.

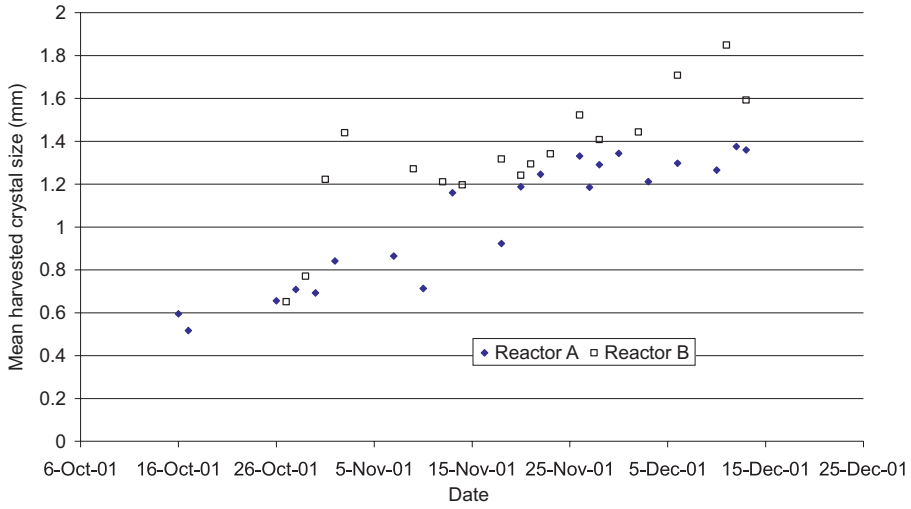

Fig. 10. Harvested crystal mass from the 1.1-L harvest zone.

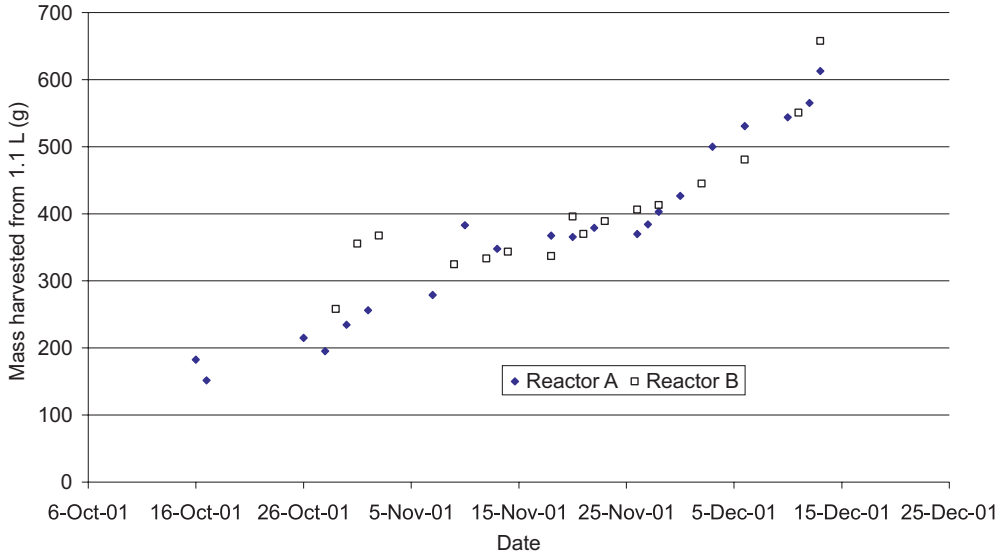

Table 2. Average results of crystal composition analysis.

% Composition by mass	Mean	Standard deviation	Theoretical value for pure struvite
Mg	9.9	0.4	9.9
N	5.6	0.3	5.7
P	12.8	0.6	12.6
Struvite (estimated)	99.8	4.0	100.0

Table 3. Struvite crystal impurity content.

% Content by weight	Mean	Standard deviation
Ca	0.49	0.32
K	0.04	0.01
Fe	0.03	0.02
Al	*	*

*Most Al analyses were below the detection limit of the method used.

increased by approximately 7 g per day of reactor operation. This increase in mass harvested coincided with the increase in diameter of the harvested crystals. Visual analysis of the crystals indicates that this increased bulk density of the crystals was probably due to the change in shape of the crystals over the course of the study, from friable plate-like aggregates to harder, rounded crystal roses.

Struvite crystal composition

To verify the composition of the crystals grown in this study, 29 samples were analyzed. Each size fraction (<0.5, 0.5–1, 1–2, and >2 mm) of harvests, from three dates from each reactor, were analyzed. Table 2 shows the average crystal compositions compared with the expected theoretical composition of pure struvite and the estimated struvite content of the crystals. The estimated struvite content was calculated by averaging the ratios of measured to theoretical composition of Mg, NH_4-N, and PO_4-P for each sample. The crystal samples were also analyzed for content of Fe, Al, K, and Ca. Based on some preliminary work, these were thought to be the most likely metals that would be found in the struvite crystals as impurities. Table 3 shows the average results. The main impurity found in the crystals was calcium, and it was present only at an average of 0.5% by weight. Based on this analysis, the produced crystals were classified as essentially pure struvite.

Microscope and scanning electron microscope crystal examination

To better understand reasons for the observed changes in harvested crystal sizes and densities, samples of the crystals were studied, first under an optical microscope at 40× magnification and then by SEM. A preliminary optical microscope observation was used to screen samples and find general trends to select representative samples for further analysis by SEM.

In general, the appearance of the crystals changed significantly with time. The early crystals appeared to be a loose aggregation of plate-like crystals, which explains why the crystals tended to break apart during the drying and screening processes. Over the course of the study, the crystals grew more rounded and more solidly aggregated. The crystals from the final harvests were very rounded and appeared to be monolithic under microscope examination at 40×.

Figure 11 shows SEM images of crystals that were retained on a 1-mm sieve, but passed a 2-mm sieve. Images (*a*), (*c*), and (*e*) are of crystals harvested from reactor A, while images (*b*), (*d*), and (*f*) are from reactor B. The bar in the bottom right of each image represents 1 mm. Images (*a*) and (*b*) are of crystals harvested in October, images (*c*) and (*d*) are of crystals harvested in November, and images (*e*) and (*f*) are of crystals harvested in December.

Fig. 11. Scanning electron microscope (SEM) images of crystals retained on a 1-mm sieve, but passing a 2-mm sieve at 50× magnification: (*a*) harvested 28 October 2001, from reactor A, (*b*) harvested 17 October from reactor B, (*c*) harvested 18 November from reactor A, (*d*) harvested 18 November from reactor B (45×), (*e*) harvested 11 December from reactor A, and (*f*) harvested 12 December from reactor B.

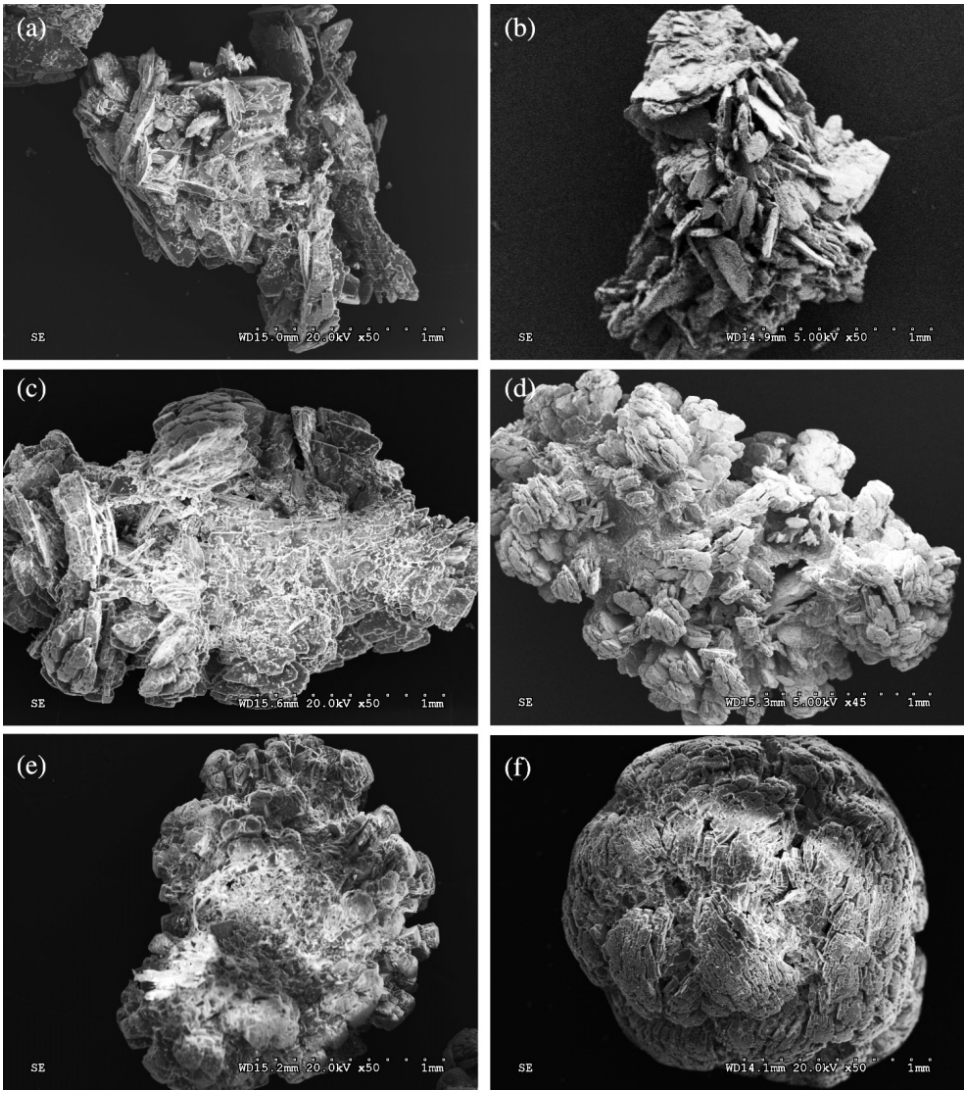

The progression in the crystal morphology is quite striking. The crystals appear to progress from loosely aggregated in October to tightly packed and more solidly bound pellets in December, especially in reactor B. The crystal from December in reactor A appears to be similar to the crystal from November in reactor B. The outside faces of these crystals (November in reactor B and December in reactor A) appear to be similar to the crystal from December in reactor B; however, their cores appear to be weaker. This may have caused the clumps of hard surface crystals to break away, either because of turbulence and impacts in the reactor or abrasion during drying and sieving operations. These images can be used to explain the difference in the bulk densities of the harvested crystals, as was discussed previously. The later crystals appear to be much rounder and more filled in, thus allowing the crystals to pack in more tightly to the harvest zone, when flow through the reactor was stopped.

In Fig. 12 crystals from the four size fractions collected on 11 December from reactor B are shown. Close inspection of Fig. 12*c* reveals that the individual surfaces on the inside of the crystal show an orthorhombic shape and are growing from the centre of the crystal outwards. This could lead to the conclusion that the stripes observed on the surface of the whole crystals may in fact be the tips of these orthorhombic crystals, which are rounded off by the abrasion in the fluidized bed and in the sieving process.

The stripes described above can be more clearly seen under higher magnification, as shown in Fig. 13. Under 300× magnification, the surface no longer appears as smooth as un-

Fig. 12. Scanning electron microscope (SEM) images of crystals harvested from reactor B on 11 December 2001: (*a*) crystal retained on a 2-mm sieve (45×), (*b*) crystal retained on a 1-mm sieve (50×), (*c*) crystals retained on a 0.5-mm sieve (45×), and (*d*) crystals passing a 0.5-mm sieve (45×).

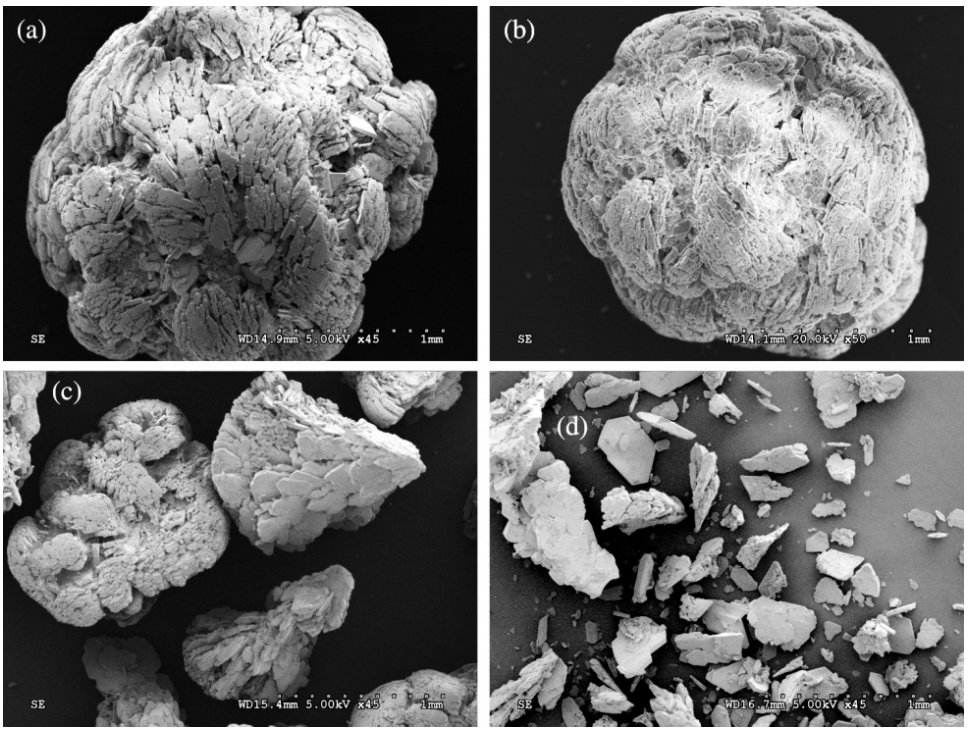

Fig. 13. Scanning electron microscope (SEM) images of a crystal retained on a 1-mm sieve, harvested from reactor B on 11 December 2001: (*a*) 50×, (*b*) 300×, and (*c*) 4000×.

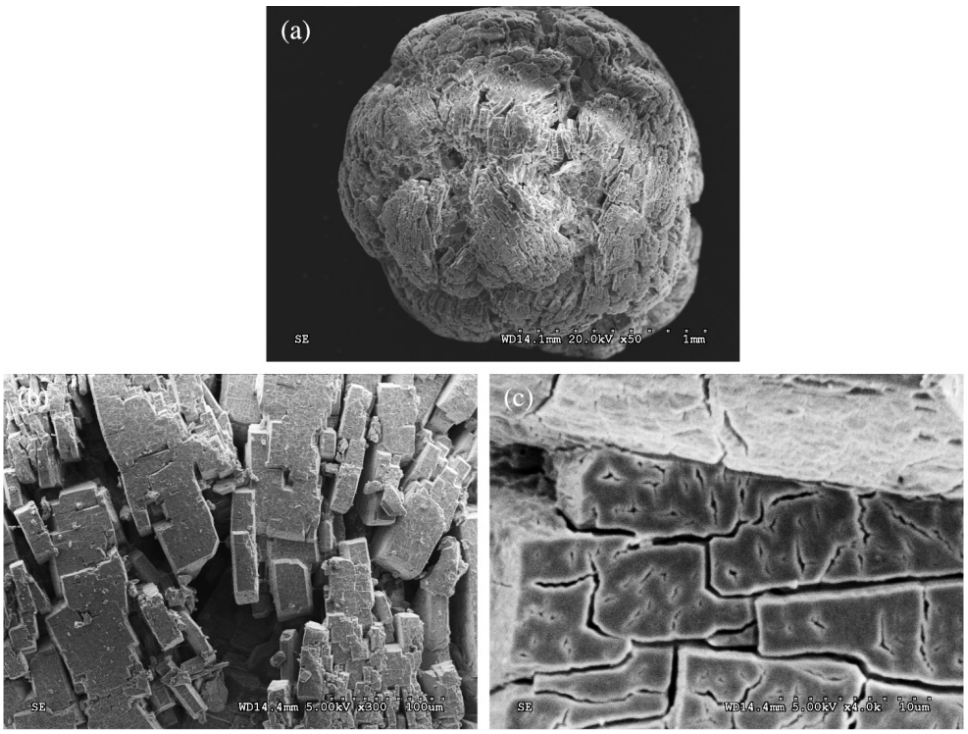

der 50× magnification, and it appears that the crystal is made up of tightly agglomerated, smaller, brick-like crystals. Under 4000× magnification, the surface of each individual crystal tip becomes more resolved, and it becomes apparent that these crystal surfaces are covered with cracks and fissures (Fig. 13).

The crystallography of the recovered crystals was not analyzed in depth but simply observed visually. Because the crystals were grown under continually varying conditions, it is impossible to determine the exact cause of the changes in the appearance of the crystals. It would also be impossible to predict the appearance of crystals from other recovery systems based on this study, especially considering that the crystals grown in this study were very different from those grown in other studies using synthetic supernatant in similar reactors (Adnan 2002; Adnan et al. 2003*b*). Further studies, under tightly controlled conditions, would probably be necessary to determine the cause-and-effect relationships leading to the final shape and size of the crystals produced.

Conclusions

Based on the results obtained from this pilot-scale study of struvite recovery from a full-scale anaerobic digester, the following conclusions can be drawn:

- The pilot-scale struvite recovery reactor developed at UBC was effective in removing orthophosphate from anaerobic digester supernatant stream under controlled conditions and produced a product consisting of nearly pure struvite.
- By controlling the operating pH of the reactors or the inlet SSR, the percentage removal of orthophosphate in the reactor varied between 42% and 91%. This study's target orthophosphate reduction of at least 70% was easily and consistently achieved.
- During the course of this study, 90% to 91% of the removed phosphorus was recovered after subsequent harvesting, drying, and screening operations.
- The size and hardness of the struvite crystals appear to have been affected by several factors, including CRT, SSR, and elapsed time from reactor start-up. It was not possible to determine the exact effect of these parameters separately from this study, because they were not varied independently.

Acknowledgements

This research project was supported financially by British Columbia Hydro and Power Authority; Stantec Consultants Ltd.; the City of Penticton, British Columbia; and the Natural Sciences and Engineering Research Council of Canada. The authors would like to especially thank the operators and technical staff at the City of Penticton AWWTP, as well as the laboratory technicians and staff at the UBC Environmental Laboratory for their support and assistance throughout this study.

References

Abe, S. 1995. Phosphate removal from dewatering filtrate by MAP process at Seibu treatment plant in Fukuoka City. Sewage Works Jpn. **43**: 59–64.

Adnan, A. 2002. Pilot-scale study of phosphorus recovery through struvite crystallization. M.Sc. thesis, Department of Civil Engineering, The University of British Columbia, Vancouver, B.C.

Adnan, A., Mavinic, D.S., and Koch, F.A. 2003*a*. Pilot-scale study of phosphorus recovery through struvite crystallization — examining the process feasibility. J. Environ. Eng. Sci. **2**: 315–324.

Adnan, A., Koch, F.A., and Mavinic, D.S. 2003*b*. Pilot-scale study of phosphorus recovery through struvite crystallization — II: Applying in-reactor supersaturation ratio as a process control parameter. J. Environ. Eng. Sci. **5**: 473–483.

APHA/AWWA/WEF. 1995. Standard met hods for the examination of water and wastewater. 19th ed. American Public Health Association, American Water Works Association, and Water Environment Federation. American Public Health Association, Washington, D.C.

Britton, A.T. 2002. Pilot-scale struvite recovery trials from a full-scale digester supernatant at the City of Penticton advanced wastewater treatment plant. M.Sc. thesis, Department of Civil Engineering, The University of British Columbia, Vancouver, B.C.

Dastur, M.B. 2001. Investigation into the factors affecting controlled struvite crystallization at the bench-scale. M.Sc. thesis, The University of British Columbia, Vancouver, B.C.

Doyle, J.D., Phillip, R., Churchley, J., and Parsons, S.A. 2000. Analysis of struvite precipitation in real and synthetic liquors. Trans. Inst. Chem. Eng., Part B, **78**: 480–488.

Driver, J., Lijmbach, D., and Steen, I. 1999. Why recover phosphorus for recycling and how? Environ. Technol. **20**: 651–662.

Jardin, N., and Popel, H.J. 1996. Behaviour of waste activated sludge from enhanced biological phosphorus removal during sludge treatment. Water Environ. Res. **68**: 965–973.

Jardin, N., and Popel, H.J. 2001. Refixation of phosphates released during bio-P sludge handling as struvite or aluminum phosphate. Environ. Technol. **22**: 1253–1262.

Mavinic, D.S., Koch, F.A., Hall, E.R., Abraham, K., and Niedbala, D. 1998. Anaerobic co-digestion of combined sludges from a biological phosphorus removal process. Environ. Technol. **19**: 35–44.

Munch, E.V., and Barr, K. 2001. Controlled struvite crystallization for removing phosphorus from anaerobic digester sidestreams. Water Res. **35**: 151–159.

Niedbala, D. 1995. Pilot-scale studies of the anaerobic digestion of combined wastewater sludges and mitigation of phosphorus release. M.Sc. thesis, The University of British Columbia, Vancouver, B.C.

Ohlinger, K.N. 1999. Struvite controls in anaerobic digestion and post-digestion wastewater treatment processes. Ph.D. thesis, University of California, Davis, Calif.

Snoeyink, V., and Jenkins, D. 1980. Water chemistry. John Wiley & Sons, New York.

Takiyama, H., Yamauchy, H., Matsuoka, M. 1997. Effects of seeding on start-up operation of a continuous crystallizer. *In* Separation and purification by crystallization. ACS Symp. Ser. **667**: 172–186.

Ueno, Y., and Fujii, M. 2001. Three years experience of operating and selling recovered struvite from full-scale plant. Environ. Technol. **22**: 1373–1381.

Woods, N.C., Sock, S.M., and Daigger, G.T. 1999. Phosphorus recovery technology modeling and feasibility evaluation for municipal wastewater treatment plants. Environ. Technol. **20**: 663–680.